

RESEARCH ARTICLE

10.1029/2018JC013884

Mesoscale Variability of Conditions Favoring an Iron-Induced Diatom Bloom Downstream of the Kerguelen Plateau

Alice Della Penna^{1,2,3,4}, Thomas W. Trull^{5,6}, Simon Wotherspoon⁷, Silvia De Monte^{8,9}, Craig R. Johnson⁷, and Francesco d'Ovidio¹

Key Points:

- Water parcels that have recently transited the Kerguelen Plateau favor diatom growth and dominance over other phytoplankton types
- Mesoscale advection of water parcels partially explains the distribution of diatom abundance and dominance in the proximity of the plateau
- The complexity of diatom dominance patterns at the mesoscale indicates that other mechanisms drive dominance further downstream

¹Sorbonne Université, UPMC Univ Paris 06, UMR 7159, LOCEAN-IPSL, Paris, France, ²Univ Paris Diderot Cité, Paris, France, ³CSIRO-UTAS Quantitative Marine Science Program, IMAS, Hobart, TAS, Australia, ⁴Applied Physics Laboratory, Air-Sea Interaction and Remote Sensing Department, University of Washington, Seattle, WA, USA, ⁵Antarctic Climate and Ecosystems Cooperative Research Centre, University of Tasmania, Hobart, TAS, Australia, ⁶CSIRO Oceans and Atmosphere, Hobart, TAS, Australia, ⁷Institute for Marine and Antarctic Studies, University of Tasmania, Hobart, TAS, Australia, ⁸Institut de biologie de l'École normale supérieure (IBENS), Département de Biologie, École normale supérieure, CNRS, INSERM, PSL Research University, Paris, France, ⁹Department of Evolutionary Theory, Max Planck Institute for Evolutionary Biology, Plön, Germany

Supporting Information:

- Supporting Information S1

Correspondence to:

A. Della Penna,
alice.dellapenna@gmail.com

Citation:

Della Penna, A., Trull, T. W., Wotherspoon, S., De Monte, S., Johnson, C. R., & d'Ovidio, F. (2018). Mesoscale variability of conditions favoring an iron-induced diatom bloom downstream of the Kerguelen Plateau. *Journal of Geophysical Research: Oceans*, 123, 3355–3367. <https://doi.org/10.1029/2018JC013884>

Received 6 FEB 2018

Accepted 9 APR 2018

Accepted article online 16 APR 2018

Published online 10 MAY 2018

Abstract Heterogeneity in phytoplankton distribution is related to spatial and temporal variations in biogeochemical and ecological processes. In the open ocean, the interaction of these processes with meso- and submeso-scale dynamics (1–100 km, few days to months) gives rise to complex spatio-temporal patterns, whose characterization is difficult without extensive sampling efforts. In this study, we integrate pigment sampling and multisatellite data to assess the link between iron enrichment and diatom dominance in the open ocean region east of the Kerguelen Islands (Indian Sector of the Southern Ocean). In this region, the High Nutrient Low Chlorophyll conditions typical of the Southern Ocean are alleviated by the transport of iron off the Kerguelen Plateau, resulting in a plume of chlorophyll that extends 1,000 km downstream. We show that in situ concentrations of the diatom-associated pigment fucoxanthin and ocean-color-derived estimates of diatom dominance correlate with the “water age”, i.e., the time since the respective water parcel departed the Kerguelen Plateau. We propose a “threshold model” linking diatom ecological success and iron availability of downstream-advected water parcels. The pattern of diatom dominance generated by this model predicts the extent and spatial structure of satellite-based estimates at the regional scale (~100s of km) and describes the mesoscale distribution of diatom dominance in the proximity of the plateau. However, the complexity of diatom dominance patterns further away from the plateau indicates that other physical and ecological mechanisms may drive phytoplankton dominance downstream.

1. Introduction

Diatoms play a crucial role in the biogeochemistry and ecology of the global ocean. They are important in several biogeochemical cycles, including carbon, iron and silicon (Armbrust, 2009; Sarthou et al., 2005; Tréguer et al., 2018). While the direct role of diatoms in carbon export is still under debate (Francois et al., 2002; Tréguer et al., 2018), diatom grazers tend to be mesozooplankton, such as copepods, amphipods and krill, that contribute considerably to carbon export by producing large fecal pellets and by vertically migrating in the water column (Turner, 2015). Therefore, diatoms and their spatio-temporal distributions are critical factors in global and regional export and the capability of the ocean to absorb CO₂. Diatoms also impact entire marine food webs, being more likely to support open ocean ecosystems that include large top predators such as marine mammals, sea birds and large fish, as well as productive fisheries (Cushing, 1989; Frederiksen et al., 2006; Hunt & McKinnell, 2006; Kiørboe, 1993; Kopczynska, 1992; Legendre, 1990; Moline et al., 2004).

The Southern Ocean is a key habitat for diatoms. It hosts the world's largest High Nutrient Low Chlorophyll region, in which production and carbon export are concentrated into areas where shallow shelf sediments, islands, sea-ice, and meltwaters from glaciers naturally fertilize the ocean with iron, the limiting nutrient for phytoplankton growth (Boyd et al., 2012; De Baar et al., 2005; Henson et al., 2012). Diatoms have been observed to be abundant in the resulting blooms (Arrigo et al., 1999; Blain et al., 2008; Smetacek et al., 2012).

Large diatoms, because of their high growth rates, thrive when iron is abundant, but are out-competed by smaller phytoplankton in iron-depleted conditions (because higher surface to volume ratios of small cells makes them more efficient at gathering iron (Hutchins et al., 1999; Sunda & Huntsman, 1995).

The spatial distribution of diatoms and other phytoplankton in these Southern Ocean blooms is often very complex, firstly because mesoscale circulation features often develop downstream from the islands and areas of shallow bathymetry where the iron enrichment occurs, and secondly because competition between different groups of primary producers and ecological successions manifest at temporal and spatial scales that overlap with the open ocean sub- and mesoscale physics (days-months, 1–100 kms). At these scales, dynamical features such as fronts and eddies produce a highly dynamic sea-scape that impacts the distribution of planktonic organisms by both shaping their habitat and advecting them (De Monte et al., 2013; d'Ovidio et al., 2010; Lehahn et al., 2007; Lévy, 2008). This dynamical complexity compounds the problems of the vastness, remoteness and harsh weather conditions of most Southern Ocean regions, because it means that the sparse in-situ biological (i.e., taxonomical observations, pigment sampling) and chemical (i.e., iron concentrations) observations cannot be readily extrapolated regionally or from one year to another. Thus, approaches that address this mesoscale complexity are important to gain insight into the mechanisms regulating Southern Ocean diatom abundances, distinguish regions characterized by different biogeochemical processes, and identify oceanic provinces that are likely to support large predators and fisheries (Allen et al., 2005; Barton et al., 2013; Dutkiewicz et al., 2009; Falkowski et al., 1998; Follows et al., 2007; Longhurst, 2010; Oliver & Irwin, 2008; Trull et al., 2015).

The goal of this study is to examine the spatial distribution of diatoms in one of the largest naturally iron-fertilized blooms of the Southern Ocean: the greater than 1,000 km long high chlorophyll plume downstream from the Kerguelen plateau and archipelago. In particular, we aim to determine to what degree mesoscale horizontal advection can be used to describe the distribution of conditions that are favorable for diatom growth. Specifically, we test the hypothesis that, in the early phase of the spring bloom, mesoscale advection is a main driver behind the spatial distribution of iron that supports diatom growth and their dominance over other phytoplankton types. To do this, we map the spatial distribution of iron using altimetry based currents (with additional wind-driven dispersion in the Ekman layer) to estimate Lagrangian water parcel trajectories, assuming that only those trajectories that cross the Kerguelen plateau are iron fertilized, and that the iron is lost over time following first order kinetics, i.e., that Fe decreases exponentially with the age of each water parcel since leaving the plateau. We compare these dynamical iron maps to information about diatom dominance at two scales: i) in waters close to the Kerguelen plateau as observed from the KEOPS2 shipboard campaign, and ii) over the entire downstream plume as estimated by the PHYSAT satellite ocean color algorithm. For the larger scale comparison, we also estimate a “threshold” iron concentration for diatom dominance, as the iron level that maximizes the pixel by pixel accuracy between the remote-sensing diatom dominance estimates and the mesoscale Lagrangian Fe maps.

2. Overview of the Study Region

The Kerguelen plateau is located in the Indian Sector of the Southern Ocean (Figure 1a). Kerguelen Island and Heard Island mark the northern and southern ends respectively, of the large and shallow central plateau ($\sim 60,000 \text{ km}^2$ at the 1,000 m isobath; Mongin et al., 2009), see Figure 1b). This area is characterized by an annual phytoplankton bloom that extends for more than $250,000 \text{ km}^2$ downstream, with chlorophyll concentrations up to 10 times that of surrounding waters. Previous studies have attributed the iron enrichment to sedimentary sources from the plateau (Blain et al., 2001, 2007, 2008; d'Ovidio et al., 2015; Quéroué et al., 2015; Trull et al., 2015; Van Der Merwe et al., 2015; Zhang et al., 2008). As in other cases of blooms developing in the wake of sub-Antarctic islands, the shape and extension of the Kerguelen bloom is known to be strongly related to the circulation (Borrione et al., 2014; d'Ovidio et al., 2015; Graham et al., 2015; Grenier et al., 2015; Mongin et al., 2008, 2009; Robinson et al., 2016; Trull et al., 2015). The local circulation is dominated by the Antarctic Circumpolar Current fronts and by the intense mesoscale activity originating from frontal instabilities and their interaction with the shallow bathymetry of the plateau (d'Ovidio et al., 2015; Park et al., 2008). Satellite images of surface chlorophyll concentrations show that the Kerguelen plume is highly heterogeneous, displaying strong gradients even within the plume itself, in response to eddies and frontal structures (Figure 1c). The community structure of the bloom's primary producers has

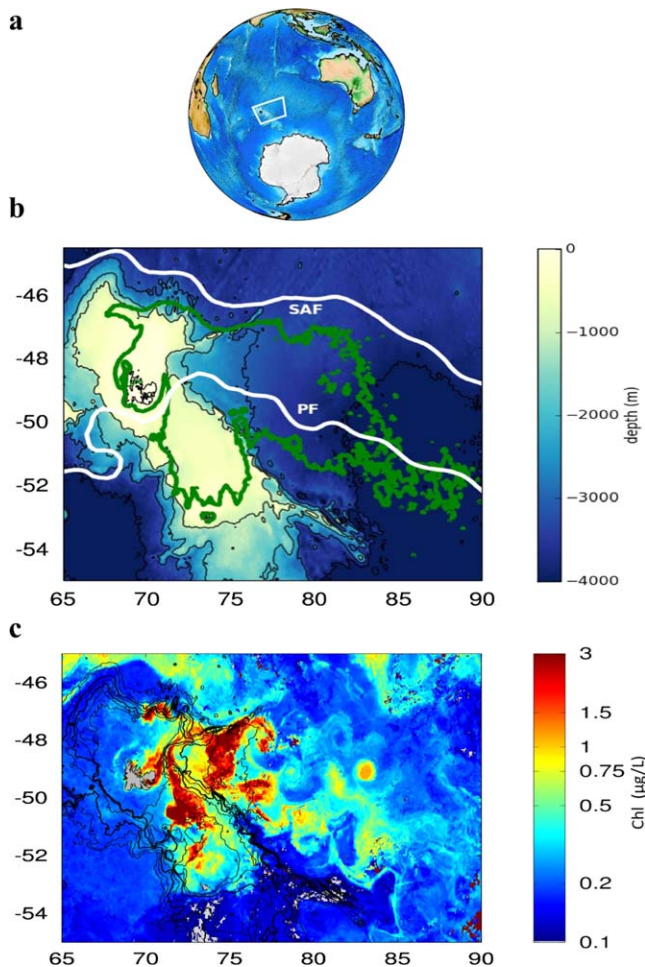


Figure 1. (a) Location of the study region in the Indian Sector of the Southern Ocean. (b) Bathymetry (color scale and black lines), overlapped with the location of the Polar (PF) and Sub-Antarctic (SAF) fronts (white), and climatological extension of the chlorophyll plume (green). The shape of the chlorophyll plume is computed by putting a threshold ($0.35 \mu\text{g/L}$) on the ocean color climatology for surface chlorophyll (calculated over spring and summer 2011–2012, corresponding to the KEOPS2 voyage). (c) Daily satellite snapshot of surface chlorophyll (11 November 2011).

study region were classified. Thus, we did not produce PHYSAT maps with mesoscale temporal and spatial resolutions, because this would be unreliable in the study region. Instead, we used PHYSAT-classified pixels in the way we would use in-situ pigment sampling observations. In this perspective, even the $<1\%$ percentage of available pixels, corresponding to more than 4,000 pixels, provides more observations than most field surveys. To carry out the comparison, we re-sampled PHYSAT observations from the months of November 2007–2010 in $20 \text{ km} \times 20 \text{ km}$ pixels. Details about the evaluation of the use of fucoxanthin as a proxy for diatoms and references to the validation of PHYSAT in the Southern Ocean can be found in supporting information S1 (Bowie et al., 2001; Hirata et al., 2011; Johnson et al., 2013; Mouw et al., 2017; Poulton et al., 2007; Wang et al., 2011).

3.2. Modeling of the Spatial Distribution of Iron Concentrations

We used a Lagrangian diagnostic called “water age” (d’Ovidio et al., 2015) as the predictor of iron concentrations. The water age quantifies the time spent away from the Kerguelen Plateau by a water parcel that has spent at least 1 day on the plateau. The plateau (here defined using the 700 m isobath as a reference – a sensitivity analysis for different isobaths and discussion about the role Mixed Layer Depth can be found in supporting information S2; Sallée et al., 2010; Van Beek et al., 2008) is considered to be a source of iron,

been studied during ship-based oceanographic campaigns, which have focused mainly on differentiating diatoms types and on pigment and size analyses (Armand et al., 2008; Lasbleiz et al., 2014, 2016; Mosseri et al., 2008; Quéguiner, 2013; Trull et al., 2015; Uitz et al., 2009). However, in-situ observations are limited in spatial extent by the large size of the plume and the remoteness of the area. Relatively little is known about phytoplankton community structure in the plume away from the Kerguelen Plateau, even though this region constitutes a productive region and an important habitat for top marine predators (Guinet et al., 2001, 2014).

3. Methods

3.1. Observations of Diatom Abundance and Dominance

Near the plateau, the spatial distribution of in situ observations of fucoxanthin concentration was used as a proxy for diatom abundance following the approach of previous works (Uitz et al., 2009; Vidussi et al., 2001; Wright et al., 1987). The pigments were collected during the *Kerguelen Ocean and Plateau compared Study 2* (KEOPS2) in November 2011. A similar analysis was performed on the microscopy based taxonomy samples collected and presented by Lasbleiz et al., (2016) and the results can be found in supporting information S4. Over the entire plume and the plateau, diatom dominance was evaluated from the PHYSAT ocean color reanalysis (Alvain et al., 2005, 2008). The PHYSAT algorithm classifies pixels of ocean color images according to an estimate of dominant phytoplankton types based on their optical properties. PHYSAT can distinguish the optical signature of six types that differ in sizes, ecological and biogeochemical roles and optical properties: nanoeukaryotes, *Prochlorococcus*, *Synechococcus*, diatoms, *Phaeocystis*, and coccolithophores. For our analysis, we selected PHYSAT observations from the month of November, when we expect the conditions in ocean physics, light and ecology to be representative of the early spring.

The PHYSAT data set is extremely sparse in the Kerguelen region: cloud coverage affects the ocean color observations PHYSAT is based on and the algorithm is not always accurate in conditions of very high and very low chlorophyll – and therefore many pixels are excluded during quality control. For these reasons, in the region of interest, during the years 2007–2010, less than 1% of the total pixels from the

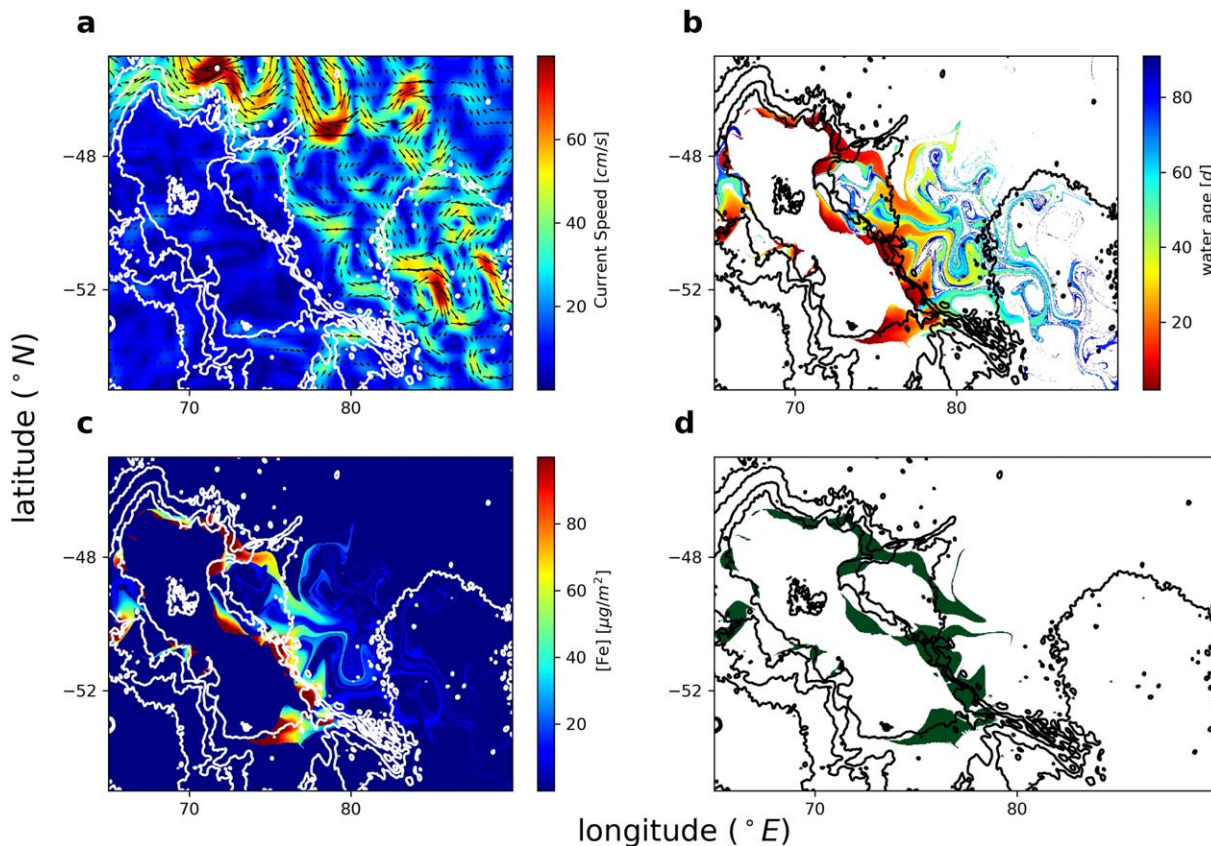


Figure 2. Conceptual scheme of the threshold model: (a) horizontal velocities derived from altimeter data are (b) integrated to compute water age. Assuming exponential loss, water age is used to calculate (c) a proxy for iron concentration, and iron concentration is then used to identify (d) areas of expected diatom dominance.

whose concentration decreases as water parcels flow downstream. “Younger” water parcels (i.e., those that have recently left the plateau) are expected to be rich in iron and favorable for diatoms. “Older” water parcels, instead, are likely to be iron depleted because of consumption by phytoplankton and abiotic scavenging (i.e., iron chemically binding to sinking particles) and therefore less likely to sustain diatoms growth and dominance. Water parcels that did not encounter the plateau in the last 3 months were considered to have an age of 90 days corresponding to the maximum backward advection time. The water age was calculated from altimetry-derived velocity fields (Figures 2a and 2b).

Specifically, the study region (latitudes = 55° to 45° S, longitudes = 65° to 90° E) was divided into 20km x 20 km pixels and for each pixel the water age and iron levels were calculated using 3 steps:

1. computing its trajectory backward in time by integrating the altimetry-derived velocity field (Figure 2a),
2. calculating the age of the water (Figure 2b),
3. quantifying a proxy for iron (Figure 2c) following the equation:

$$\frac{dFe}{dt} = -k Fe \quad (1)$$

where k represents the iron loss rate. Since in different seasons iron loss can be dominated by different processes, we separated k into k_1 and k_2 while integrating equation (1). k_1 and k_2 represent iron loss rates associated with times of the year when abiotic scavenging and phytoplankton consumption respectively dominate iron loss. These rates have been estimated as $k_1 = 0.041d^{-1}$ and $k_2 = 0.058 d^{-1}$ by measuring dissolved iron (i.e., the form of iron that is more likely to be available for phytoplankton growth) during different seasons (d’Ovidio et al., 2015). The values of k_1 and k_2 are also consistent with the estimates of iron

export in free-floating traps (Laurenceau et al., 2014). These two values reflect different phases of water parcel history, with k_1 applying to late winter conditions when iron loss is mainly due to abiotic scavenging and k_2 representative of spring, when iron loss is augmented by consumption by phytoplankton, so that:

$$t_1 + t_2 = \text{water age} \quad (2)$$

The quantity of available dissolved iron for a water parcel can be computed as:

$$[Fe] = [Fe_0] e^{-(k_1 * t_1 + k_2 * t_2)} \quad (3)$$

where $Fe_0 = 150 \mu\text{mol m}^{-2}$ has been also estimated by d'Ovidio et al. (2015) by integrating plateau's measurements of dissolved iron over the top 150 m.

3.3. Comparison of the Modeled Iron Distributions and Diatom Dominance Maps

For the ship based diatom dominance observations, we compared the fucoxanthin and water age based results for Fe levels using a Pearson's correlation coefficient. For the satellite observations, the water age of the water parcels occupying each pixel having a valid PHYSAT observation was calculated and compared with the phytoplankton dominance (i.e., diatom-dominated or not) of the respective pixel by using a General Additive Model (GAM). This comparison is based on the level of Fe modeled for each pixel from the circulation and Fe loss model (section 2.3) and the assumption of a "threshold" level of Fe that ensures diatom dominance, i.e., assuming that water parcels having more iron than a certain threshold available will be diatom dominated and the others will be dominated by other phytoplankton types. We selected the threshold iron concentration that determines diatom dominance as the one that maximized the model accuracy –i.e., the fraction of PHYSAT pixels that are correctly predicted by the model. For the selected threshold, the output of the threshold model (Figure 2d) was compared to the PHYSAT observations in terms of false positives, false negatives, true positives, true negatives. We assessed the spatial distribution of these diagnostics by computing maps of the most likely result (accurate prediction, false positive, false negative) that the model gives at predicting PHYSAT observations at different locations. More generally, we studied the output of the GAM by analyzing the ranges of the probability of observing diatom dominance for water parcels of different ages, the trends in diatom dominance versus age, and their rates of change. We also evaluated the predictive value of the obtained statistical model by using the area under the curve of the Receiver Operating Characteristic (ROC) (Fawcett, 2004). The area under the curve of the ROC of a classifying model is defined as a number between 0 and 1, where 1 indicates the performance of a perfect model and 0.5 a random model.

3.4. Assumptions of Our Approach

The Kerguelen bloom lasts for a few months and extends for thousands of kilometers. In this study, we focus on the early bloom, when we expect the following assumptions to be satisfied:

1. bottom-up ecological effects: iron abundance is the sole resource determining the success of diatoms. Light or other nutrients (such as silicates; Mosseri et al., 2008; Quéguiner, 2013) are assumed not to be limiting for diatoms, and generally phytoplankton, growth. Diatoms establish their dominance by competitive exclusion of other phytoplankton types (i.e., diatoms are either dominant or non-dominant at a given time and location; Collie et al., 2004; Hardin, 1960; May, 1977)
2. role of bathymetry and ocean dynamics: the main source of iron is the Kerguelen Plateau (here defined as the 700 m isobath- a sensitivity analysis for the choice of the isobath can be found in supporting information S2.). Water enriched on the plateau is horizontally advected according to altimetry-derived geostrophic currents (with additional spreading in the Ekman layer as driven by winds as detailed in supporting information S2; Roach et al., 2015). The used velocity field does not explicitly capture the sub-mesoscale and may be overly smooth since it is based on altimetry (Keating et al., 2012) but has the advantage of avoiding possible model biases and the misplacement of physical structures such as fronts and eddies. Advection is assumed to dominate the transport of iron over diffusion as suggested by previous studies (Mongin et al., 2009).
3. biogeochemistry: iron loss is proportional to its concentration (i.e., first order loss), with more rapid loss during the spring blooming than during winter. The motivation for two different time constants comes from the overall length-scale of the bloom which suggests lower loss rates in winter (Mongin et al., 2009)

than suggested by the decrease in dFe concentrations with water parcel ages in summer (d'Ovidio et al., 2015).

4. top-down ecological effects: grazing by zoo-plankton and loss by sedimentation are in fixed proportion to phytoplankton growth rates, so that biomass accumulation scales with phytoplankton growth rates, without preferential effects on community composition.

These assumptions and their limitations are revisited in the Discussion section. Further details of the different data and methods (including details of the advection scheme (Hernández-Carrasco et al., 2011), in-situ data, satellite products used, etc.) are presented in the supporting information S1.

4. Results

4.1. Identification of Fucoxanthin Spatial Distribution

The spatial variability of fucoxanthin concentrations (dots in Figure 3) spans one order of magnitude, indicating a possibly large variability in diatom concentrations on a scale of a few hundreds of kilometers. The fucoxanthin distribution does not display any clear zonal or meridional gradient. Along the KEOPS2 east-west sampling axis, fucoxanthin is high at the very proximity of the plateau, decreases to a minimum concentration about one order of magnitude smaller near 72–73° E, and increases toward the stations farther from the plateau. A similar structure can be found in the north-south axis, suggesting that there is a specific area that is less favorable for diatoms than the immediate surroundings. This pattern cannot be directly linked with the geographical distance from the Kerguelen Plateau. But we do find good agreement with the “water age”, with fucoxanthin decreasing in older waters (Figure 3, Pearson’s correlation coefficient = -0.66 , p -value = $5 \cdot 10^{-4}$). High fucoxanthin concentrations in “young” water parcels suggest that they are particularly favorable for diatoms (Figure 3). A similar trend can be found in samples studied microscopically for phytoplankton taxonomy in the region (supporting information S4).

4.2. Water Age as an Environmental Driver of Dominance: Trends, Probabilities, and Rate

The GAM model fitting each PHYSAT observation with its respective water age is:

$$probability(\text{diatoms dominance}) \sim s(\text{age}) \quad (3)$$

where $s(\text{age})$ is the GAM smooth function ($p < 2 \cdot 10^{-16}$) displayed in Figure 5a. The probability of observing diatom dominance is ~ 0.67 for water parcels relatively close to the plateau (age ~ 2 days). This probability decreases at an approximately constant rate for the first 40–50 days to a probability of 0.45 that is associated to water parcels up to 60 days of age and then it decreases to values of 0.23 to fit the water parcels

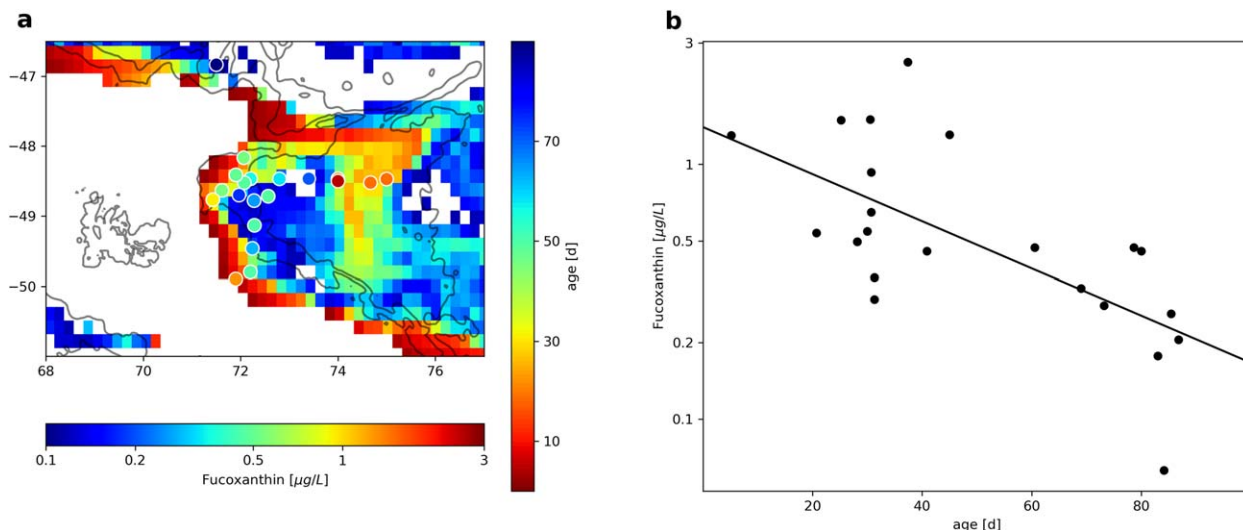


Figure 3. (a) Spatial distribution of fucoxanthin measured in water samples overlapped with a November 2011 climatology of water age (estimated using Lagrangian analysis). Visual inspection suggests that fucoxanthin concentrations decline with the time since water was in contact with the plateau. (b) Plot of empirical fucoxanthin against estimated water age confirms the negative relationship (corr = -0.66 , $P = 5 \cdot 10^{-4}$).

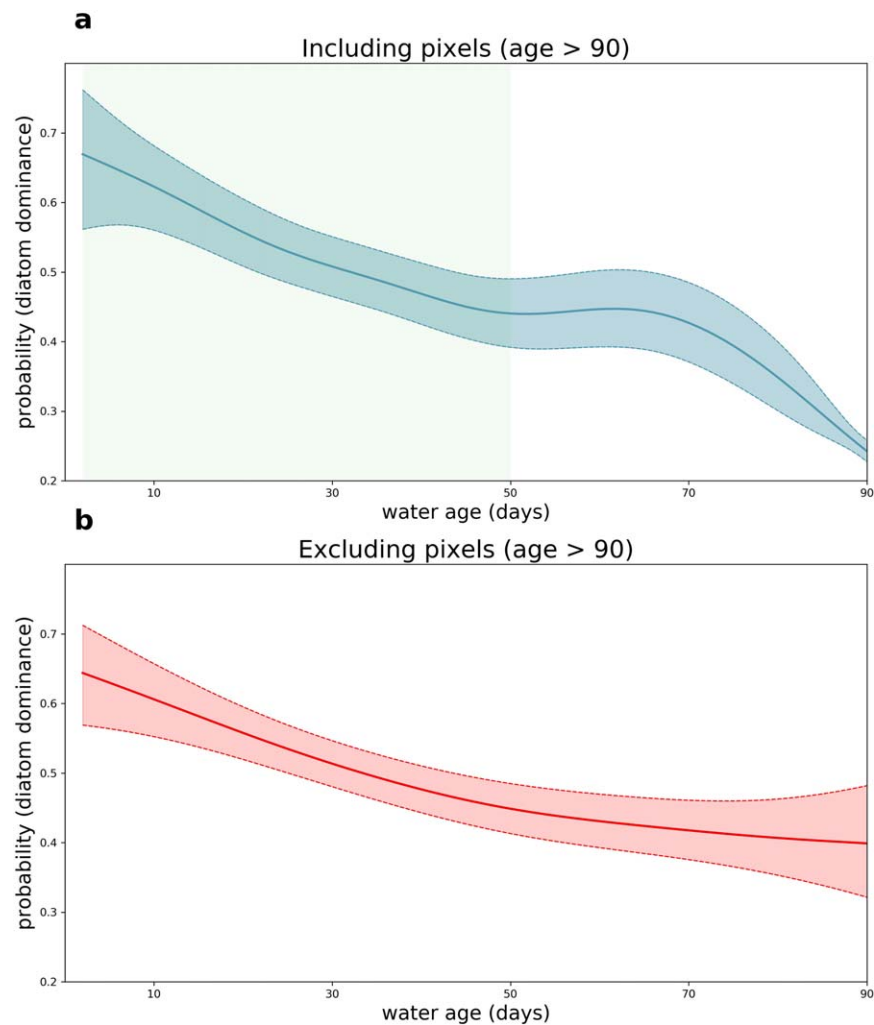


Figure 4. Smooth functions for the GAM statistical models showing the relation between probability of observing diatom dominance and age of water parcels. The GAM smooth function in Figure 4a is fitted using all the available PHYSAT pixels. The one in Figure 4b is calculated excluding pixels that have not encountered the Kerguelen Plateau 90 days prior to the respective PHYSAT observation. Shaded curves indicate confidence intervals and the green shading in Figure 4a highlights the interval of water ages used to estimate the decrease rate.

that have never encountered the plateau in the last 90 days. In general, for all water ages, the variability (expressed for example as the confidence intervals of the GAM on Figure 4) is large and ranges from 0.05–0.2. Higher variability is associated to water parcels near the plateau or water parcels with ages ~ 90 days. Lower variability is associated to water parcels that did not cross the plateau in the last 90 days. The rate of loss of probability of diatom dominance for the first 50 days (highlighted by a green shading in Figure 4a) is 0.021 d^{-1} . The smooth function of the GAM fitted excluding water parcels that have not encountered the plateau in the last 90 days (Figure 4b) presents the same shape as the one of the GAM including water parcels older than 90 days (Figure 4a) for ages up to 50 days. However, it presents different probabilities for water parcels of water ages between 60–90 days (0.45 versus 0.23). The area under the curve of the ROC calculated for this GAM model is 0.64.

4.3. Reconstructing Diatom Biogeography From Ecology and Transport: Threshold Model and Spatial Patterns

The threshold in iron values that maximizes the accuracy (0.69) corresponds to a value of vertically integrated iron concentration of $23 \mu\text{mol m}^{-2}$. Because this value is tied to the assumed plateau initial $[\text{Fe}_0]$ value of $150 \mu\text{mol m}^{-2}$, the important result is not its absolute value, but rather that the threshold model suggests diatom dominance continues until only 23 parts in 150 of the initial Fe remains (15%).

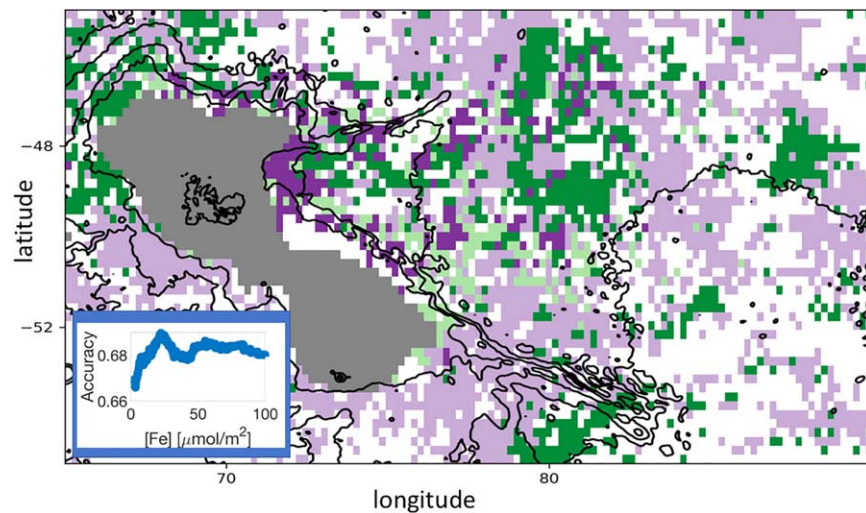


Figure 5. Spatial distribution of the threshold model's performance. White refers to pixel with no available PHYSAT observation. Dark and light purple pixels indicate true negatives and true positives respectively. Light green pixels indicate false positives (i.e., regions where the threshold model predicted a diatom dominance that was not observed in PHYSAT) and dark green pixels indicate false negatives (i.e., regions where the model failed at predicting observed diatom dominance). The inset shows the variability of the accuracy of the threshold model for different values of the threshold in dissolved iron concentration.

For the threshold value of $23 \mu\text{mol m}^{-2}$ the model produces 403 true positives (9%), 2,647 true negatives (60%), 348 false positives (8%) and 1,030 false negatives (23%). The distribution of model success varies spatially. It predicts successfully the PHYSAT observations that are available south-west of the Kerguelen Plateau, most of the values north of the plume downstream, south-east of the plateau and in the areas close to the northern plateau where the pigment samples were collected (Figure 5—in purple). False positives (i.e., pixels where the model predicted a diatom dominance that was not observed by PHYSAT) are present patchily within the downstream plume (Figure 5—in light green). False negatives (i.e., pixels where the model failed to predict an observed diatom dominance) are remarkably clustered in two regions: north-west of the plateau and in correspondence of the Williams Ridge, south-east of the plateau (Figure 5—in dark green).

5. Discussion

5.1. Does Horizontal Advection of Iron Affect Diatom Abundance and Dominance Near the Kerguelen Plateau?

Our shipboard and satellite results indicate that, even though during shipboard studies diatoms have been observed ubiquitously in the proximity of the Kerguelen Plateau, the spatial distribution of their abundance and dominance of phytoplankton assemblage is patchy (Figure 3a). This spatial variability can be interpreted within the framework of Lagrangian approaches applied previously in this area (d'Ovidio et al., 2015; Mongin et al., 2009; Sanial et al., 2014). The significant relationship between fucoxanthin concentration measured in situ and estimated water ages suggests that iron scavenging and consumption affect the suitability of water parcels for diatom growth (Figure 3b).

The pixel-based GAM statistical model highlights the decrease of probability of observing diatom dominance as water parcels age as they travel away from the plateau (Figure 4). The trend is consistent with our hypothesis that mesoscale advection is crucial in structuring the spatial distribution of diatoms dominance over other phytoplankton types. This result is consistent with previous works that found that meso and sub-mesoscale features affect phytoplankton abundance and community structure in models (Bracco et al., 2000; Lévy, 2003; Lévy et al., 2001; Perruche et al., 2011) and observations (Abraham, 1998; d'Ovidio et al., 2010) by structuring the distribution of nutrients and also separating competing groups (Bracco et al., 2000; Perruche et al., 2011).

5.2. Does Horizontal Advection of Iron Affect Diatom Abundance and Dominance Away From the Plateau?

After the first 50 days of water parcel ages, the shape of the GAM smooth function (Figure 4a) changes and the probability of observing diatom dominance is approximately constant for water parcels of water ages between 50 and 70 days (diatom dominance probability of 0.45 in comparison to the initial value of 0.67). 0.45 is the mean probability that water parcels that have touched the plateau have and also the probability for water parcels of ages > 50 days in the GAM fit, if water parcels that have not encountered the plateau in the last 90 days are excluded (Figure 4b). If these pixels are included, as in Figure 4a and in our analysis, the probability for water parcels of age ~ 90 days drops to 0.23. If horizontal mesoscale advection and competitive exclusion for iron were the only controlling mechanisms for dominant phytoplankton types the probabilities would range from 0 to 1 and not from 0.23 to 0.67. This suggests that, while mesoscale currents are definitely related to distribution of diatoms abundance and dominance, other mechanisms, unresolved in this approach, introduce a high variability in the system. The high variability identified in this study may also be affected by the limitations related to identifying diatom dominance from space: in order to clearly disentangle all the different mechanisms affecting diatom dominance and abundance more fieldwork is likely to be needed.

5.3. Why Are Not All Young Water Parcels Dominated by Diatoms?

The 0.67 probability for water parcels that have left the plateau is likely to be caused by differences in the initial phytoplankton community on the plateau itself. Our approach is based on the assumption that on the plateau, where iron is expected to be abundant, diatoms always dominate the community and always in similar proportion. Pigment sampling (Lasbleiz et al., 2014) and Remote Access Sampling (RAS) (S. Blain, personal communication, 2017) suggest that diatoms often do dominate the phytoplankton community on the plateau. However, PHYSAT observations indicate that even on the plateau in the beginning of the bloom other groups such as *Synechococcus* and nano-eukaryotes dominate the community. It is possible that these inferred different communities are an artifact introduced by the use of PHYSAT over shallow bathymetry, where ocean color images may be dominated by inorganic particles. Alternatively, the variations in phytoplankton dominance may be real and linked to differential iron enrichment (due to different locations of enrichment or to the different amount of time that water parcels spend on the plateau – see supporting information S3 for more details), or other controls on phytoplankton community structure such as light levels (possibly controlled by varying mixed layer depths that climatologies suggest can range between 50–100 m on different parts of the Kerguelen Plateau (supporting information S2; Sallée et al., 2010). Finally, it is important to remark that the detection of a previous contact with the plateau as well as the estimation of the water age is derived by a Lagrangian advection scheme calculated from the altimetric velocity field. Although this approach has been validated by comparison with isotope measurements and extensive comparison with more than 50 real drifters (d'Ovidio et al. 2015; Sanial et al. 2014), some spurious contact detection may be possible both because of errors in the advection schemes and because of the resolution of the velocity field. As a consequence, some water parcels may have a (wrongly) estimated young age and no diatom dominance, reducing the overall probability of diatom dominance for young water parcels.

5.4. Why Does Diatom Dominance Occur in Some Old Water Parcels Whose Fe Levels Should be Below the Threshold Value?

The 0.23 probability of diatom dominance in water parcels or with water ages ~ 90 days (Figure 4a) could result from additional sources of iron. In particular, submesoscale stirring has been hypothesized to induce vertical movements and potentially resupply iron to surface iron-depleted waters. Both analysis of horizontal velocities from altimetry and models indicate that the region east of Kerguelen is characterized high eddy kinetic energy (d'Ovidio et al., 2015; Rosso et al., 2014; Tamsitt et al., 2016). Another possibility is ecological succession of different types of diatoms with different iron requirements (i.e., different threshold values). PHYSAT generically identifies diatoms without distinguishing between different types. Quéguinier (2013) compared observations from natural and artificial iron fertilization and suggested that diatoms having large size, high growth rates, and rapid onset of limitation by iron and other nutrients dominates the phytoplankton biomass at the beginning of the spring bloom, and are then succeeded in summer by smaller diatoms with lower maximum growth rates but higher efficiency of Fe uptake at low concentration (as well as greater resistance to grazing). This seasonal succession might manifest as spatial variations in the PHYSAT images, given that water parcels enriched in the northern part of the plateau are transported

southeastward downstream. Another point worth mentioning is that the error on the calculation on water parcel trajectories (and thus the derived diagnostics) grows as the time of advection increases (Özgökmen et al., 2000). This means that, in a pixel-by-pixel comparison such as the one used to produce Figure 4, we can be more confident that we are associating a PHYSAT observation to its correct water age in regions where water parcels are generally young (with the caveat that the uncertainty on water parcel trajectories grows differently for different dynamical regimes). While a comparison between climatologies of water age computed using altimetry-derived currents and Lagrangian drifters in the study region suggests that pattern in water ages computed in the two cases are remarkably similar even far downstream the Kerguelen Plateau (d'Ovidio et al., 2015), it is possible that the 0.23 probability for water parcels that have crossed the plateau more than 90 days prior to observations is calculated including water parcels that were enriched more recently and were not correctly matched to their respective PHYSAT observation.

5.5. Is There a Unique Threshold for Diatom Dominance?

The optimal threshold for the model is $23 \mu\text{mol m}^{-2}$ iron, corresponding to the 15% of the initial enrichment. While these numbers are consistent with previous estimates from artificial iron enrichment experiments, i.e., \sim equivalent to 0.2 nM Fe in a 100 m deep mixed layer and thus similar to the level enrichment that engendered rapid increases in biomass accumulation during SOIREE and other enrichments (Boyd et al., 2001, 2007), it should be considered with caution. The inset in Figure 5 highlights that the accuracy of the threshold model is not particularly sensitive to the value of the threshold itself, suggesting that, if the entire region is considered, it may be more important for a water parcel to be enriched on the plateau at all, rather than having a particular threshold level of Fe. The limitations of a single threshold are also made clear by the observed gradual exponential decrease of diatom dominance with water age (Figure 4), rather than a step change at the threshold value. This gradual decrease may arise for many reasons, e.g.:

- i. differing extents of initial iron enrichment (i.e., water parcels get to the threshold at different times because some started with more iron, by being enriched in different parts of the plateau or by spending more time on shallow isobaths – see supporting information S3),
- ii. different loss rates, i.e., some water parcels are slower at reaching the threshold than others. Indeed, our model's assumption of two separate time constant for Fe loss in winter and spring predicts that parcels in the age range of 40–50 days will either be diatom dominated or not depending on when they left the plateau and not just on their age. Remineralization may also slow down the iron loss as water age increases, especially if loss rates decrease with biomass analogously to f-ratios and export losses (e.g., Laws et al., 2000).

It is also possible that the ecological dynamics of the planktonic community in water parcels 'inoculated' with a community dominated by large diatoms may manifest inertia to transition to a community dominated by small non-diatom phytoplankton. In other words, the dynamics of the planktonic community in this region could be characterized by ecological hysteresis (Begon, 1996). In this scenario, a community initially dominated by large diatoms and subject to declining iron concentrations would transition to domination by other phytoplankton types (e.g., nanophytoplankton) at much lower iron levels than would be expected to manifest as nanophytoplankton dominance when the initial 'inoculum' was dominated by nanophytoplankton.

A single threshold approach is unlikely to grasp all the complexity of the system, but it provides a useful starting point. With our current state of knowledge, it is difficult to determine whether a threshold is necessary at all. However, using this approach to discriminate between regions of different phytoplankton dominance provides a heuristic comparison to theory and complementary data sets.

5.6. The Threshold Model Performance and Its Spatial Variability

The predictive performance of the threshold model (ROC = 0.64) indicates that it should not be used indiscriminately to predict the dominant type of a pixel-sized region. Indeed, while we can be reasonably confident that a pixel that the model predicts to be non-diatom dominated will be classified "correctly" (i.e., consistently with PHYSAT), a pixel that is predicted by the model to be diatom-dominated has only 0.5 probability to be observed to be dominated by diatoms by PHYSAT.

The spatial distribution of false positives and false negatives highlighted in Figure 5 suggests that within the plume PHYSAT identifies a variety of pixels as non-diatom dominated (false positives). False negatives

appear to be clustered north-west of the plateau, where waters may have been enriched in the proximity of the Crozet archipelago and have been advected downstream and southward to the northern part of the Kerguelen plateau, and in correspondence of Williams ridge –the narrow bathymetric feature ~80 E, –53 S. Such region is likely to be characterized by vertical movement of water as the total kinetic energy of the mesoscale flow is generally high (Rosso et al., 2014).

Improving our understanding of the departures from the simple threshold model is likely to require further fieldwork. In particular, it would be extremely valuable to collect taxonomical information or pigment samples and ocean physics conditions in regions where PHYSAT and the threshold model consistently disagree (e.g., near Williams ridge) and more generally to determine how different Fe supply mechanisms and community composition controls are entwined in different parts of the study region.

6. Conclusions

The results of this study suggest that mesoscale advection correlates with trends in fucoxanthin concentrations and PHYSAT observations. Younger water parcels, recently enriched in iron by crossing the plateau, correspond to higher fucoxanthin concentrations and are more likely to indicate dominance by diatoms in remotely sensed observations. Notably, the water-age based description captures successfully the extent and the shape of the mesoscale recirculation feature near the northern part of the Kerguelen Plateau which has unexpectedly low diatom dominance (and unexpectedly low phytoplankton biomass (d'Ovidio et al., 2015; Trull et al., 2015)). The shape of the statistical relationship between water age and observed dominance, model performance based on the pixel-by-pixel GAM, and the performance of the threshold model, suggest that while iron supplied from horizontal mesoscale advection is likely to be an essential factor in determining favorability for diatom growth and their dominance over other phytoplankton groups, other mechanisms will need to be considered to develop a high-performance predictive model.

Acknowledgments

The altimeter products were produced by Ssalto/Duacs and distributed by Aviso with support from CNES and from the Collecte Localisation Satellites (CLS). The authors wish to thank Jean Baptiste Sallé for the Mixed Layer Depths estimates, Isabelle Pujol (CLS) for her help with the regional altimetry products, Stéphan Blain for his help with the access to the pigment data and useful discussions and Severine Alvain for her suggestions about the use of PHYSAT. ADP thanks the Fondation Bettencourt-Schueller (through the program Frontières du Vivant) and the Quantitative Marine Science Program (CSIRO-UTAS) for financial support during her Ph.D. project. SDM acknowledges support of the CNRS-PSL Eco-Evo-Devo program "Pepinière Interdisciplinaire" and the program « Investissements d'Avenir » launched by the French Government and implemented by ANR with the references ANR-10-LABX-54 MEMOLIFE and ANR-10-IDEX-0001-02 PSL* Research University. TWT's participation was supported by the Australian Commonwealth Cooperative Research Centre Program. This work has been partly supported by the Tosca-Cnes LAECOS project. The authors would like to thank three anonymous reviewers for their constructive criticisms. Altimetry data are available on the AVISO altimetry webpage (<https://www.aviso.altimetry.fr/>). Chlorophyll maps are available on the GlobColour platform (<http://www.globcolour.info/>). PHYSAT ocean color re-analyses are available on the GlobColour platform or on PHYSAT's official webpage (<http://log.cnrs.fr/Physat-2?lang=fr>). Pigment in situ observations can be obtained requesting an access to (<http://keops2.obs-vlfr.fr/>) or from the publication by Lasbleiz et al. (2016).

References

- Abraham, E. R. (1998). The generation of plankton patchiness by turbulent stirring. *Nature*, *391*, 577–580.
- Allen, J. T., Brown, L., Sanders, R., Moore, C. M., Mustard, A., Fielding, S., . et al. (2005). Diatom carbon export enhanced by silicate upwelling in the North-east Atlantic. *Nature*, *437*, 728–732.
- Alvain, S., Le Quéré, C., Bopp, L., Racault, M. F., Beaugrand, G., Dessailly, D., & Buitenhuis, E. T. (2013). Rapid climatic driven shifts of diatoms at high latitudes. *Remote Sensing of Environment*, *132*, 195–201.
- Alvain, S., Loisel, H., & Dessailly, D. (2012). Theoretical analysis of ocean color radiances anomalies and implications for phytoplankton groups detection in case 1 270 waters. *Optics Express*, *20*(2), 1070–1083.
- Alvain, S., Moulin, C., Dandonneau, Y., & Breon, F. M. (2005). Remote sensing of phytoplankton groups in case 1 waters from global SeaWiFS imagery. *Deep Sea Research Part I: Oceanographic Research Papers*, *52*, 1989–2004.
- Alvain, S., Moulin, C., Dandonneau, Y., & Loisel, H. (2008). Seasonal distribution and succession of dominant phytoplankton groups in the global ocean: A satellite view. *Global Biogeochemical Cycles*, *22*, GB3001. <https://doi.org/10.1029/2007GB003154>
- Armand, L. K., Cornet-Barthaux, V., Mosseri, J., & Quéguiner, B. (2008). Late summer diatom biomass and community structure on and around the naturally iron fertilised Kerguelen plateau in the Southern Ocean. *Deep Sea Research, Part II: Topical Studies in Oceanography*, *55*, 653–676.
- Armbrust, E. V. (2009). The life of diatoms in the world's oceans. *Nature*, *459*(7244), 185.
- Arrigo, K. R., Robinson, D. H., Worthen, D. L., Dunbar, R. B., DiTullio, G. R., VanWoert, M., & Lizotte, M. P. (1999). Phytoplankton community structure and the drawdown of nutrients and CO₂ in the Southern Ocean. *Science*, *283*(5400), 365–367.
- Barton, A. D., Pershing, A. J., Litchman, E., Record, N. R., Edwards, K. F., Finkel, Z. V., et al. (2013). The biogeography of marine plankton traits. *Ecological Letters*, *16*, 522–534.
- Begon, M., (1996). Harper, J., & Townsend, *Ecology: Individuals, populations and communities* (3rd. ed.). Oxford, UK: Blackwell Science.
- Blain, S., Quéguiner, B., Armand, L., Belviso, S., Bombled, B., Bopp, L., et al. (2007). Effect of natural iron fertilization on carbon sequestration in the Southern Ocean. *Nature*, *446*, 1070–1074.
- Blain, S., Quéguiner, B., & Trull, T. (2008). The natural iron fertilization experiment KEOPS (KErguelen Ocean and Plateau compared Study): An overview. *Deep Sea Research, Part II: Topical Studies in Oceanography*, *55*, 559–565.
- Blain, S., Tréguer, P., Belviso, S., Bucciarelli, E., Denis, M., Desabre, S., et al. (2001). A biogeochemical study of the island mass effect in the context of the iron hypothesis: Kerguelen islands, Southern Ocean. *Deep Sea Research, Part I: Oceanographic Research Papers*, *48*, 163–187.
- Borrione, I., Aumont, O., Nielsdottir, M., & Schlitzer, R. (2014). Sedimentary and atmospheric sources of iron around South Georgia, Southern Ocean: A modelling perspective. *Biogeochemistry*, *11*, 1981–2001.
- Bowie, A. R., Maldonado, M. T., Frew, R. D., Croft, P. L., Achterberg, E. P., Mantoura, R. F. C., et al. (2001). The fate of added iron during a meso-scale fertilisation experiment in the Southern Ocean. *Deep Sea Research, Part II: Topical Studies in Oceanography*, *48*(11), 2703–2743.
- Boyd, P., Abraham, E., & Streppek, R. (2001). Iron-mediated changes in phytoplankton photosynthetic competence during SOIREE. *Deep-Sea Research, Part II: Topical Studies in Oceanography*, *48*, 2529–2550.
- Boyd, P. W., Arrigo, K. R., Strzepek, R., & Dijken, G. L. (2012). Mapping phytoplankton iron utilization: Insights into Southern Ocean supply mechanisms. *Journal of Geophysical Research*, *117*, C06009. <https://doi.org/10.1029/2011JC007726>
- Boyd, P. W., Jickells, T., Law, C. S., Blain, S., Boyle, E. A., Buesseler, K. O., et al. (2007). Mesoscale iron enrichment experiments 1993–2005: Synthesis and future directions. *Science*, *315*, 612–617.

- Bracco, A., Provenzale, A., & Scheuring, I. (2000). Mesoscale vortices and the paradox of the plankton. *Proceedings of the Royal Society London, Series B: Biological Sciences*, *267*, 1795–1800.
- Collie, J. S., Richardson, K., & Steele, J. H. (2004). Regime shifts: Can ecological theory illuminate the mechanisms?. *Progress in Oceanography*, *60*, 281–302.
- Cushing, D. H. (1989). A difference in structure between ecosystems in strongly stratified waters and in those that are only weakly stratified. *Journal of Plankton Research*, *11*(1), 1–13.
- De Baar, H. J., Boyd, P. W., Coale, K. H., Landry, M. R., Tsuda, A., Assmy, P., et al. (2005). Synthesis of iron fertilization experiments: From the iron age in the age of enlightenment. *Journal of Geophysical Research*, *110*, C09S16. <https://doi.org/10.1029/2004JC002601>
- De Monte, S., Soccodato, A., Alvain, S., & D'ovidio, F. (2013). Can we detect oceanic biodiversity hotspots from space?. *The ISME Journal*, *7*(10), 2054–2056.
- D'Ovidio, F., Della Penna, A., Trull, T. W., Nencioli, F., Pujol, I., Rio, M. H., et al. (2015). The biogeochemical structuring role of horizontal stirring: Lagrangian perspectives on iron delivery downstream of the Kerguelen Plateau. *Biogeosciences*, *12*(1), 779–814.
- D'ovidio, F., Monte, S. D., Alvain, S., Dandonneau, Y., & Lévy, M. (2010). Fluid dynamical niches of phytoplankton types. *Proceedings of the National Academy of Sciences of the United States of America*, *107*, 18366–18370.
- Dutkiewicz, S., Follows, M. J., & Bragg, J. G. (2009). Modeling the coupling of ocean ecology and biogeochemistry. *Global Biogeochemical Cycles*, *23*, GB4017. <https://doi.org/10.1029/2008GB003405>
- Falkowski, P. G., Barber, R. T., & Smetacek, V. (1998). Biogeochemical controls and feedbacks on ocean primary production. *Science*, *281*, 200–206.
- Fawcett, T. (2004). ROC graphs: Notes and practical considerations for researchers. *Machine Learning*, *31*, 1.
- Follows, M. J., Dutkiewicz, S., Grant, S., & Chisholm, S. W. (2007). Emergent biogeography of microbial communities in a model ocean. *Science*, *315*, 1843–1846.
- Francois, R., Honjo, S., Krishfield, R., & Manganini, S. (2002). Factors controlling the flux of organic carbon to the bathypelagic zone of the ocean. *Global Biogeochemical Cycles*, *16*(4), 1087. <https://doi.org/10.1029/2001GB001722>
- Frederiksen, M., Edwards, M., Richardson, A. J., Halliday, N. C., & Wanless, S. (2006). From plankton to top predators: Bottom-up control of a marine food web across four trophic levels. *Journal of Animal Ecology*, *75*(6), 1259–1268.
- Graham, R. M., De Boer, A. M., van Sebille, E., Kohfeld, K. E., & Schlosser, C. (2015). Inferring source regions and supply mechanisms of iron in the Southern Ocean from satellite chlorophyll data. *Deep Sea Research, Part I: Oceanographic Research Papers*, *104*, 9–25.
- Grenier, M., Della Penna, A., & Trull, T. (2015). Autonomous profiling float observations of the high biomass plume downstream of the Kerguelen Plateau in the Southern Ocean. *Biogeosciences*, *11*(12), 17413–17462.
- Guinet, C., Dubroca, L., Lea, M., Goldsworthy, S., Cherel, Y., Duhamel, G., et al. (2001). Spatial distribution of foraging in female antarctic fur seals *Arctocephalus gazella* in relation to oceanographic variables: A scale-dependent approach using geographic information systems. *Marine Ecology Progress Series*, *219*, 251–264.
- Guinet, C., Vacqu e-Garcia, J., Picard, B., Bessigneul, G., Lebras, Y., Dragon, A.-C., et al. (2014). Southern elephant seal foraging success in relation to temperature and light conditions: Insight into prey distribution. *Marine Ecology Progress Series*, *499*, 285–301.
- Hardin, G. (1960). The competitive exclusion principle. *Science*, *131*, 1292–1297.
- Henson, S. A., Sanders, R., & Madsen, E. (2012). Global patterns in efficiency of particulate organic carbon export and transfer to the deep ocean. *Global Biogeochemical Cycles*, *26*, GB1028. <https://doi.org/10.1029/2011GB004099>
- Hern andez-Carrasco, I., L opez, C., Hern andez-Garc a, E., & Turiel, A. (2011). How reliable are finite-size Lyapunov exponents for the assessment of ocean dynamics? *Ocean Modelling*, *36*(3), 208–218.
- Hirata, T., Hardman-Mountford, N., Brewin, R., Aiken, J., Barlow, R., Suzuki, K., et al. (2011). Synoptic relationships between surface chlorophyll-a and diagnostic pigments specific to phytoplankton functional types. *Biogeosciences*, *8*(2), 311–327.
- Hunt, G. L., & McKinnell, S. (2006). Interplay between top-down, bottom-up, and wasp-waist control in marine ecosystems. *Progress in Oceanography*, *68*(2), 115–124.
- Hutchins, D. A., Witter, A. E., Butler, A., & Luther, G. W. (1999). Competition among marine phytoplankton for different chelated iron species. *Nature*, *400*(6747), 858–861.
- Johnson, R., Stratton, P. G., Wright, S. W., McMinn, A., & Meiners, K. M. (2013). Three improved satellite chlorophyll algorithms for the Southern Ocean. *Journal of Geophysical Research: Oceans*, *118*, 3694–3703. <https://doi.org/10.1002/jgrc.20270>
- Keating, S. R., Majda, A. J., & Smith, K. S. (2012). New methods for estimating ocean eddy heat transport using satellite altimetry. *Monthly Weather Review*, *140*(5), 1703–1722.
- Kj orboe, T. (1993). Turbulence, phytoplankton cell size, and the structure of pelagic food webs. *Advances in Marine Biology*, *29*, 1–72.
- Kopczynska, E. E. (1992). Dominance of microflagellates over diatoms in the antarctic areas of deep vertical mixing and krill concentrations. *Journal of Plankton Research*, *14*, 1031–1054.
- Lasbleiz, M., Leblanc, K., Armand, L. K., Christaki, U., Georges, C., Obernosterer, I., & Qu eguiner, B. (2016). Composition of diatom communities and their contribution to plankton biomass in the naturally iron-fertilized region of Kerguelen in the Southern Ocean. *FEMS Microbiology Ecology*, *92*(11),
- Lasbleiz, M., Leblanc, K., Blain, S., Ras, J., Cornet-Barthaux, V., H elias Nunige, S., & Qu eguiner, B. (2014). Pigments, elemental composition (C, N, P, and Si), and stoichiometry of particulate matter in the naturally iron fertilized region of Kerguelen in the southern ocean. *Biogeosciences*, *11*(20), 5931–5955.
- Laurenceau, E. C., Trull, T. W., Davies, D. M., Bray, S. G., Doran, J., Planchon, F., et al. (2014). The relative importance of phytoplankton aggregates and zooplankton fecal pellets to carbon export: Insights from free-drifting sediment trap deployments in naturally iron-fertilised waters near the Kerguelen Plateau. *Biogeosciences*, *11*, 13623–13673.
- Laws, E. A., Falkowski, P. G., Smith, W. O. J., Ducklow, H., & McCarthy, J. J. (2000). Temperature effects on export production in the open ocean. *Global Biogeochemical Cycles*, *14*, 1231–1246.
- Legendre, L. (1990). The significance of microalgal blooms for fisheries and for the export of particulate organic carbon in oceans. *Journal of Plankton Research*, *12*(4), 681–699.
- Lehahn, Y., D'ovidio, F., L evy, M., & Heifetz, E. (2007). Stirring of the Northeast Atlantic spring bloom: A Lagrangian analysis based on multi-satellite data. *Journal of Geophysical Research*, *112*, C08005. <https://doi.org/10.1029/2006JC003927>
- L evy, M. (2003). Mesoscale variability of phytoplankton and of new production: Impact of the large-scale nutrient distribution. *Journal of Geophysical Research*, *108*(C11), 3358. <https://doi.org/10.1029/2002JC001577>
- L evy, M. (2008). *The modulation of biological production by oceanic mesoscale turbulence* (pp. 219–261). In *Transport and mixing in geophysical flows* (pp. 219–261). Berlin, Heidelberg: Springer.

- Lévy, M., Klein, P., & Treguier, A.-M. (2001). Impact of sub-mesoscale physics on production and subduction of phytoplankton in an oligotrophic regime. *Journal of Marine Research*, *59*, 535–565.
- Longhurst, A. (2010). *Ecological geography of the sea*. Cambridge, MA: Academic Press.
- May, R. M. (1977). Thresholds and breakpoints in ecosystems with a multiplicity of stable states. *Nature*, *269*, 471–477.
- Moline, M. A., Claustre, H., Frazer, T. K., Schofield, O., & Vernet, M. (2004). Alteration of the food web along the Antarctic Peninsula in response to a regional warming trend. *Global Change Biology*, *10*(12), 1973–1980.
- Mongin, M., Molina, E., & Trull, T. W. (2008). Seasonality and scale of the Kerguelen plateau phytoplankton bloom: A remote sensing and modeling analysis of the influence of natural iron fertilization in the Southern Ocean. *Deep Sea Research, Part II: Topical Studies in Oceanography*, *55*(5), 880–892.
- Mongin, M. M., Abraham, E. R., & Trull, T. W. (2009). Winter advection of iron can explain the summer phytoplankton bloom that extends 1000 km downstream of the Kerguelen plateau in the southern ocean. *Journal of Marine Research*, *67*, 225–237.
- Mosseri, J., Queguiner, B., Armand, L., & Cornet-Barthaux, V. (2008). Impact of iron on silicon utilization by diatoms in the southern ocean: A case study of Si/N cycle decoupling in a naturally iron-enriched area. *Deep Sea Research, Part II: Topical Studies in Oceanography*, *55*, 801–819.
- Mouw, C. B., Hardman-Mountford, N. J., Alvain, S., Bracher, A., Brewin, R. J., Bricaud, A., et al. (2017). A consumer's guide to satellite remote sensing of multiple phytoplankton groups in the global ocean. *Frontiers in Marine Science*, *4*, 41. <https://doi.org/10.3389/fmars.2017.00041>
- Oliver, M. J., & Irwin, A. J. (2008). Objective global ocean biogeographic provinces. *Geophysical Research Letters*, *35*, L15601. <https://doi.org/10.1029/2008GL034238>
- Özgökmen, T. M., Griffa, A., Mariano, A. J., & Piterbarg, L. I. (2000). On the predictability of Lagrangian trajectories in the ocean. *Journal of Atmospheric and Oceanic Technology*, *17*(3), 366–383.
- Park, Y.-H., Roquet, F., Durand, I., & Fuda, J.-L. (2008). Large-scale circulation over and around the northern Kerguelen Plateau. *Deep Sea Research, Part II: Topical Studies in Oceanography*, *55*, 566–581.
- Perruche, C., Riviere, P., Lapeyre, G., Carton, X., & Pondaven, P. (2011). Effects of surface quasi-geostrophic turbulence on phytoplankton competition and coexistence. *Journal of Marine Research*, *69*, 105–135.
- Poulton, A. J., Moore, C. M., Seeyave, S., Lucas, M. I., Fielding, S., & Ward, P. (2007). Phytoplankton community composition around the Crozet Plateau, with emphasis on diatoms and Phaeocystis. *Deep Sea Research, Part II: Topical Studies in Oceanography*, *54*(18), 2085–2105.
- Quéguiner, B. (2013). Iron fertilization and the structure of planktonic communities in high nutrient regions of the Southern Ocean. *Deep Sea Research Part II: Topical Studies in Oceanography*, *90*, 43–54.
- Quéroué, F., Sarthou, G., Planquette, H., Bucciarelli, E., Chever, F., Van Der Merwe, P., et al. (2015). High variability in dissolved iron concentrations in the vicinity of the Kerguelen Islands (Southern Ocean). *Biogeosciences*, *12*(12), 3869–3883.
- Roach, C. J., Phillips, H. E., Bindoff, N. L., & Rintoul, S. R. (2015). Detecting and characterizing Ekman currents in the Southern Ocean. *Journal of Physical Oceanography*, *45*(5), 1205–1223.
- Robinson, J., Popova, E. E., Srokosz, M. A., & Yool, A. (2016). A tale of three islands: Downstream natural iron fertilization in the Southern Ocean. *Journal of Geophysical Research: Oceans*, *121*, 3350–3371. <https://doi.org/10.1002/2015JC011319>
- Rosso, I., Hogg, A. M., Strutton, P. G., Kiss, A. E., Matear, R., Klocker, A., & van Sebille, E. (2014). Vertical transport in the ocean due to sub-mesoscale structures: Impacts in the Kerguelen region. *Ocean Modelling*, *80*, 10–23.
- Sallée, J.-B., Speer, K., & Rintoul, S. (2010). Zonally asymmetric response of the Southern Ocean mixed-layer depth to the Southern Annular Mode. *Nature Geoscience*, *3*(4), 273–279.
- Sanial, V., van Beek, P., Lansard, B., D'ovidio, F., Kestenare, E., Souhaut, M., et al. (2014). Study of the phytoplankton plume dynamics off the Crozet islands (Southern Ocean): A geochemical-physical coupled approach. *Journal of Geophysical Research: Oceans*, *119*, 2227–2237. <https://doi.org/10.1002/2013JC009305>
- Sarthou, G., Timmermans, K. R., Blain, S., & Tréguer, P. (2005). Growth physiology and fate of diatoms in the ocean: A review. *Journal of Sea Research*, *53*(1), 25–42.
- Smetacek, V., Klaas, C., Strass, V. H., Assmy, P., Montresor, M., Cisewski, B., et al. (2012). Deep carbon export from a Southern Ocean iron-fertilized diatom bloom. *Nature*, *487*(7407), 313–319.
- Sunda, W. G., & Huntsman, S. A. (1995). Iron uptake and growth limitation in oceanic and coastal phytoplankton. *Marine Chemistry*, *50*(1–4), 189–206.
- Takao, S., Hirawake, T., Wright, S. W., & Suzuki, K. (2012). Variations of net primary productivity and phytoplankton community composition in the Indian sector of the Southern Ocean as estimated from ocean color remote sensing data. *Biogeosciences*, *9*(10), 3875.
- Tamsitt, V., Talley, L. D., Mazloff, M. R., & Cerovečki, I. (2016). Zonal variations in the Southern Ocean heat budget. *Journal of Climate*, *29*(18), 6563–6579.
- Tréguer, P., Bowler, C., Moriceau, B., Dutkiewicz, S., Gehlen, M., Aumont, O., et al. (2018). Influence of diatom diversity on the ocean biological carbon pump. *Nature Geoscience*, *11*(1), 27.
- Trull, T. W., Davies, D. M., Dehairs, F., Cavagna, A.-J., Lasbleiz, M., Laurenceau, E. C., et al. (2015). Chemometric perspectives on plankton community responses to natural iron fertilization over and downstream of the Kerguelen Plateau in the Southern Ocean. *Biogeosciences*, *11*, 13841–13903.
- Turner, J. T. (2015). Zooplankton fecal pellets, marine snow, phytodetritus and the ocean's biological pump. *Progress in Oceanography*, *130*, 205–248.
- Uitz, J., Claustre, H., Griffiths, F. B., Ras, J., Garcia, N., & Sandroni, V. (2009). A phytoplankton class-specific primary production model applied to the Kerguelen islands region (Southern Ocean). *Deep Sea Research, Part I: Oceanographic Research Papers*, *56*, 541–560.
- Van Beek, P., Bourquin, M., Reyss, J. L., Souhaut, M., Charette, M. A., & Jeandel, C. (2008). Radium isotopes to investigate the water mass pathways on the Kerguelen Plateau (Southern Ocean). *Deep Sea Research, Part II: Topical Studies in Oceanography*, *55*(5), 622–637.
- Van Der Merwe, P., Bowie, A. R., Quéroué, F., Armand, L., Blain, S., Chever, F., et al. (2015). Sourcing the iron in the naturally fertilised bloom around the Kerguelen Plateau: Particulate trace metal dynamics. *Biogeosciences*, *12*(3), 739–755.
- Vidussi, F., Claustre, H., Manca, B. B., Luchetta, A., & Marty, J. C. (2001). Phytoplankton pigment distribution in relation to upper thermocline circulation in the eastern Mediterranean Sea during winter. *Journal of Geophysical Research: Oceans*, *106*, 19939–19956.
- Wang, S., & Moore, J. K. (2011). Incorporating Phaeocystis into a Southern Ocean ecosystem model. *Journal of Geophysical Research*, *116*, C01019. <https://doi.org/10.1029/2009JC005817>
- Wright, Simon, W., S. W. & Jeffrey, (1987). Fucoxanthin pigment markers of marine phytoplankton analysed by HPLC and HPTLC. *Marine Ecology Progress Series*, 259–266.
- Zhang, Y., Lacan, F., & Jeandel, C. (2008). Dissolved rare earth elements tracing lithogenic inputs over the Kerguelen Plateau (Southern Ocean). *Deep Sea Research Part II: Topical Studies in Oceanography*, *55*(5–7), 638–652.